# The influence of N₂ flow on the micro-structure and corrosion resistance of TaN coatings on bipolar plates for PEM electrolyser

**Jianping Gao**[1, 2, †], **Yuangjiang Lv**[1, †], **Yongjing Li**[1], **Wenqian Sun**[1], **BiYing Ren**[2],

**Zhengfei Dai**[1], **Fei Ma**[1, *]

[1] *State Key Laboratory for Mechanical Behavior of Materials, Xi'an Jiaotong University, Xi'an 710049, Shaanxi, China*

[2] *Western Metal Materials Co., Ltd., Xi'an, 710201, Shaanxi, China*

[†] *These authors have contributed equally to this work*

**Abstract:** Corrosion shortens the service period of bipolar plates (BPs) and increases the costs of proton exchange membrane water electrolyser (PEMWE). In this work, TaN coatings are deposited on Ti BPs by magnetron sputtering to improve the corrosion resistance and service period, and the influences of N₂ flow on the surface morphology, hydrophobicity, crystallinity, corrosion resistance and interfacial contact resistance of TaN coatings are studied in details. As the N₂ flow increases, the roughness of TaN coatings decreases firstly and then increases in accordance with the hydrophobicity. At the N₂ flow of 3 sccm, TaN coating with the larger grain size presents the lower roughness and hydrophobicity. As a result, the coating possesses the lowest $I_{corr}$ of 2.82 µA·cm⁻² and the highest $E_{corr}$ of -0.184 V vs. SCE in the simulated PEMWE environment. After 10 h potentiostatic polarization test, fewer corrosion pits are observed on the TaN coatings deposited at the 3 sccm N₂ flow. Hence, the TaN coating on BPs could improve the corrosion resistance properties and thus enhance the electrolysis efficiency (68.87%) in the tested single electrolytic cell after 75 h.

**Key words:** TaN coatings, corrosion resistance, Ti bipolar plate, water electrolysis

Proton exchange membrane water electrolyser (PEMWE) is one of the important strategies for solving the issues of environmental pollution[1,2]. The bipolar plates (BPs), one of the key components of PEMWE, provide structural support for the membrane electrode assembly (MEA), distribute water across the porous transportlayer, conducte electrons between cells and facilitate the mass transport and thermal management. Compared with stainless steel (SS), titanium-based BPs exhibit outstanding corrosion resistance, high electric and thermal conductivity, excellent mechanical strength[3]. Anode side titanium bipolar plates used in these applications typically employ coatings of platinum group metals to achieve durability and performance requirements in the high voltage, oxidizing environment. The high corrosion resistance of titanium favors the chemical stability of proton exchange membrane and catalyst. However, BPs occupy 30% of the PEMWE cell cost and >60% of its weight[4], and corrosion is the main failure of BPs[5,6]. Therefore, anti-corrosion coatings

have been explored to enhance the corrosion resistance of BPs and prolong the service life[4,7,8]. In addition, the passivation film formed on the metal surface usually results in the elevated interfacial contact resistance (ICR) between the BPs and the porous transport layer (PTL)[9]. The oxide layer formed during electrolysis will also increase ICR values. This will lead to a significant decline of electrolysis efficiency and the shortened service life.

Commonly, metallic nitrides with strong ionic bonds exhibit high anti-corrosion properties and are usually applied to protect BPs[10-14]. For instance, CrN coatings deposited on stainless steel (SS) BPs presented high corrosion resistance with a low corrosion current density ($I_{corr}$<0.26 μA·cm$^{-2}$)[15,16]. However, C/Al doped-CrN coatings showed the degraded corrosion resistance with the higher $I_{corr}$ (>0.277 μA·cm$^{-2}$ and even 0.576 μA·cm$^{-2}$). NbN and TiN coatings on Ti BPs presented the excellent corrosion resistance with $I_{corr}$<0.73 μA·cm$^{-2}$ and low ICR<15.8 mΩ cm$^2$[14,17]. TaN (607 kJ·mol$^{-1}$) has the higher bond dissociation energy than those of TiN (476 kJ·mol$^{-1}$) and NbN (226 kJ·mol$^{-1}$)[16], and should exhibit the better corrosion resistance, but TaN coatings are seldomly focused[19,20].

In this paper, TaN coatings are deposited on Ti BPs via the direct current magnetron sputtering. The influences of N$_2$ flow on the surface morphology, phases, roughness, water contact angle, as well as o the corrosion and ICR properties of TaN coatings are studied in details. The anti-corrosion mechanism is uncovered.

# 1 Coating preparation and characterization

## 1.1 Materials preparation

Prior to coating deposition, pure Ti specimens are ground with 800#, 1500# and 2500# SiC papers, and then ultrasonically cleaned with alcohol and deionized water for 15 min, respectively, finally placed in a low temperature and dust-free environment for natural drying. TaN coatings are deposited on the Ti substrates by reactive sputter-deposition technique (JGP450). The base pressure is 5×10$^{-5}$ Pa. Ar (99.999%) plasma is used to remove the impurities and oxides on the targets and substrate surfaces. Ta target (99.995%, Φ=50 mm) is used as the metal source with the distance between the target and the substrate of 150 mm, while N$_2$ gas (99.999% purity) is used as the N source. The N$_2$ flow is 2, 3, 4 and 5 sccm with the Ar flow of 20 sccm. The work pressure, direct current power, deposition time and deposition temperature are set as 0.7 Pa, 80 W, 1.5 h and 150 °C, respectively.

## 1.2 Material characterizations

X-ray diffraction patterns (XRD, Bruker/D8 Advance, Germany, (λ=0.15405 nm)) of TaN coatings are measured in the scaning range of 20~80° at an operation voltage of 40 kV and an operation current of 30 mA, respectively. The surface and cross-section morphologies are characterized by field emission scanning electron microscope (FESEM, JSM-7001F,

JEOL Ltd, Tokyo, Japan), equipped with energy-dispersive spectroscopy (EDS), atan operation voltage of 15 kV and an operation current of 25 pA. The roughness is tested by Confocal Laser Scanning Microscope (Olympus, OLS5100). The surface wettability of the coatingsis investigated by measuring the static contactangle (θ) atthe ambient temperature, atmospheric pressure and relative humidity of 45%. The contact angle is measured using 2 mL water droplet by contact angle measuring apparatus.

## 1.3 Electrochemical measurement

Potentiodynamic polarizationis performed inan electrochemical cell consisting of a three-electrode test system using a platinum sheet as counter electrode and a saturated calomel electrode (SCE) connected to a luggin capillary filled with saturated KCl solution as reference electrode. TaN coatings on Ti are served as the working electrode. The potentiodynamic and potentiostatic polarization tests of TaN coatings are done in the PEMWE simulated acidic aqueous environment (0.5 mol/L H$_2$SO$_4$ + 2 ppm F$^-$) at 80 °C via the electrochemical workstation (Autolab-PGSTAT 128 N). The potentiodynamic polarization test is done from -1.0 V to 2.5 V vs. RHE at a scanning rate of 1 mV·S$^{-1}$ after the 1 hour open-circuit potential (OCP), while the potentiostatic polarization operates under 2 V.

## 1.4 Interfacial contact resistance (ICR) measurement

The ICR between the specimen surface and a porous transport layer (PTL) is determined by PEM fuel cell test method. The sample is placed between two pieces of conductive carbon paper (Toray TGP-H-090), and then sandwiched between two Au-coated copperplates. The applied current is stabilized at 1.5 A with the compaction force on the two Au-coated copper plates increasing from 0.1 to 2.0 MPa gradually. The corresponding voltage is recorded to calculate the total resistance as a function of compaction force. The resistance of the carbon papers is measured in the same way and subsequently subtracted from the total resistance[12]. The ICR values at a conventional compaction pressure of 1.5M Paisan evaluation index of electrical conductivity between different samples.

## 1.5 Electrolyser tests

A PEM electrolyser cell consisting of multi-channel flow field Ti BPs is manufactured with an active surface area of 70 mm × 120 mm. The TaN coating is deposited on anode BPs by magnetron sputtering, as described in Section 2.1. The sintered Ti fiber felts coated with 500nm Pt by electroplating are used as the porous transport layer (PTL) of anode and cathode. A commercially available membrane electrode assembly (MEA) is utilized, which consists of a Nafion 115 membrane, Ir-based anode catalyst and Pt-based cathode catalyst, and the catalyst loading is 1.0 mg·cm$^{-2}$ and 0.5 mg·cm$^{-2}$, respectively. A testing station for the PEM electrolyser measurements is assembled, including programmable power supply module, gas-water separators,

computer control module and thermostatic circulating water module. Ultrapure water (conductivity <5 µS·cm⁻¹) is used, which is heated up to 80 ℃ and supplied to the anode side by a peristaltic pumpat a flow rate of 400 ml·min⁻¹.

## 2 Results and Discussion

### 2.1 The XRD patterns of TaN coatings prepared at different N₂ flows

Fig. 1 shows the XRD patterns of TaN coatings prepared at different N₂ flows.As the N₂ flow is increased from 2 sccm to 4 sccm, the crystallinity of TaN coating is improved, with the preferred TaN (111) orientation. The XRD peaks at 35.83°, 41.46°, 60.26° and 72.12° are indexed to the (111), (200), (220) and (311) planes of cubic TaN phase. However, as the N₂ flow is further increased to 5 sccm, the crystallinity of TaN coatings decreases, and even becomes amorphous. The N atomic content increases with the N₂ flow gradually increase, and reaches at 55.64 at.% at 5 sccm N₂ flow, as indicted by the EDS results in Table 1[14,21]. For reactive sputtering, as the nitrogen flow is increased, the collision probability between sputtered Ta atoms and the plasma will be increased, and thus the sputtered Ta atoms carry less kinetic energy, and the bombardment of Ta and N atoms on Ti substrates as well as on the coatings is weaker. This leads to slower nucleation of the coating and smaller nuclei. Specifically, when the stoichiometric ratio of N to Ta exceeds 1:1 (the N percentage of 55.64 at.% in Table 1), the atoms with lower kinetic energy pile up into an amorphous structure.

**Table 1 The EDS of TaN coatings prepared at different N₂ flows**

| Sample | Ta at./% | N at./% |
|---|---|---|
| 2 sccm N₂ flow | 47.78 | 52.22 |
| 3 sccm N₂ flow | 46.89 | 53.11 |
| 4 sccm N₂ flow | 46.58 | 53.42 |
| 5 sccm N₂ flow | 44.36 | 55.64 |
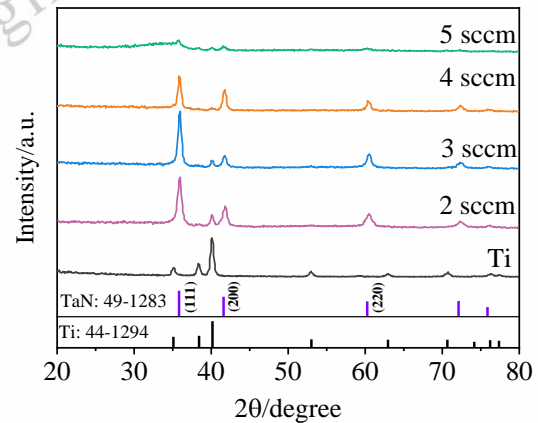


Fig. 1 XRD patterns of TaN coatings prepared at different N₂ flows

### 2.2 The surface roughness and hydrophobicity of TaN coatings

Fig. 2a1-d1 show the sample morphology of TaN coatings observed by confocal laser scanning microscope, and they exhibit smooth morphology with the color changing from brown to gray, which can be ascribed to the different surface roughness and crystalstructure[22]. Fig. 2a2-d2 show the grayscale images of surface roughness, the average arithmetic roughness (Sa) are 0.054 µm, 0.036 µm, 0.052 µm and 0.052 µm, respectively. The TaN coating prepared at 3 sccm N₂ flow has the smallest roughness,with fewer pits and gullies, which could prolong the service life of BPs[14,23]. As illustrated in Fig. 2a3-d3, the water contact angles of TaN coatingsare above 90°, indicating hydrophobicity, and the TaN coating prepared at 3 sccm N₂ flow presents the lowest hydrophobicity.
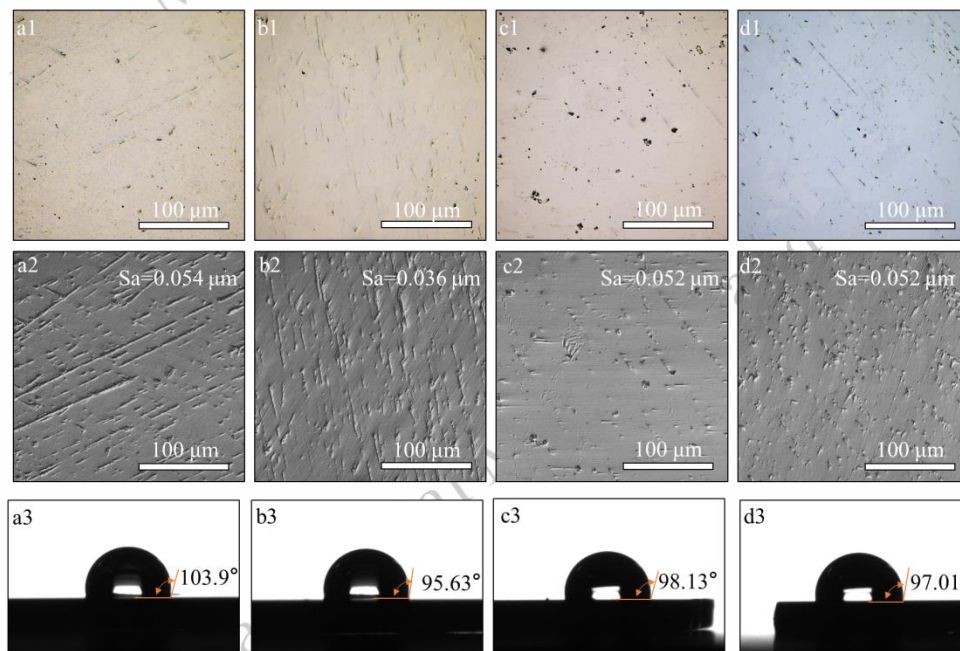


Fig. 2 (a1)-(d1) micro-surface morphology, (a2)-(d2)surface roughness and (a3)-(d3) water contact angles of TaN coatings prepared at the N₂ flows

of 2, 3, 4 and 5 sccm, repectively.

## 2.3 The surface morphology of TaN coatings

Fig. 3 shows the cross-section and surface morphology of TaN coatings. As displayed in Fig. 3a1-d1, the coatings are composed of columnar-like grains, and the thickness decreases with $N_2$ flow increase. Since the ionization energy of N is higher than that of Ar, the plasma is reduced with increasing $N_2$ flow, and thus the depositon of TaN is slowed down. Fig. 3a2-d3 show the surface morphology of the coatings, and Fig.

3a4-d4 exhibit the grain size distribution. For the coatings deposited at $N_2$ flow of 2 and 3sccm, the surface morphology is smooth with larger grain sizes (Fig. 3a2-b3). However, if the $N_2$ flow is further increased to 4 and 5 sccm, the surface morphology becomes rougher with some ridges and particles (Fig. 3c2 and d2). Meanwhile, the average grain size decreases (Fig. 3c4 and d4).
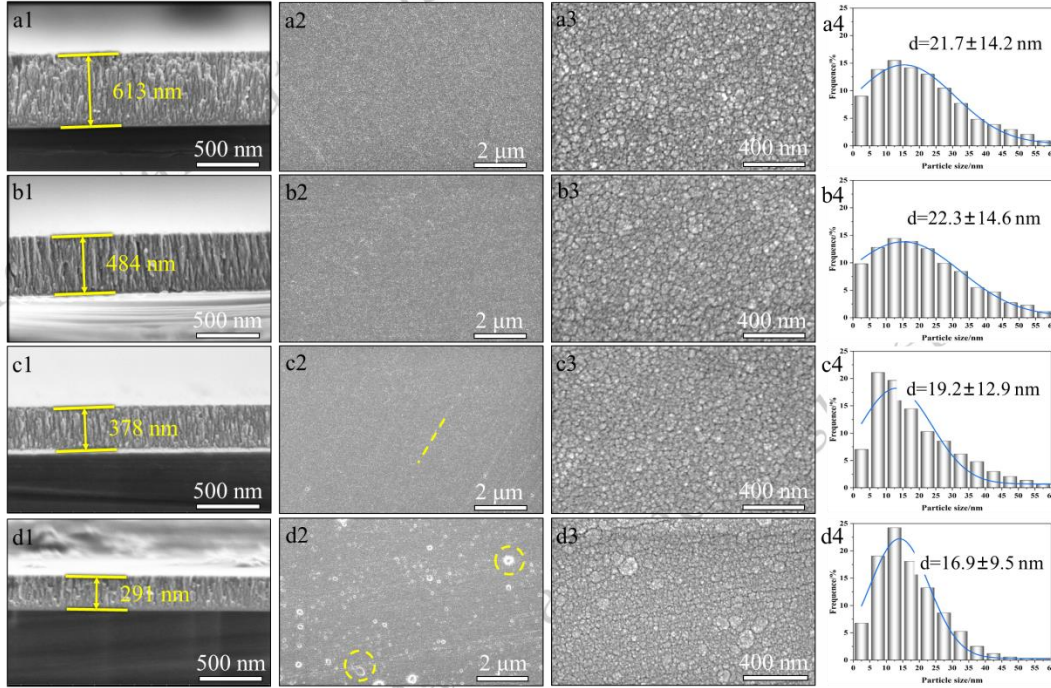


Fig. 3 The cross-section, surface morphology and grain size distribution ofTaNcoatings prepared at the different $N_2$ flows: (a1)-(a4) at 2sccm, (b1)-(b4) at 3sccm, (c1)-(c4) at 4sccm and (d1)-(d4) at 5sccm.

## 2.4 The corrosion resistance of TaN coatings

The cathodic Tafel slope ($\beta_c$) and anodic Tafel slope ($\beta_a$) are obtained through linear fitting the cathode and anodic Tafel regions of the corrosion polarization curves. And the intersection of cathode Tafel fitting curve and anode Tafel fitting curve is self-corrosion current density ($I_{corr}$) and corrosion potential ($E_{corr}$). The polarization resistance (Rp) calculated by Eq. (1)[24].

$$R_p = \frac{\beta_a \times \beta_c}{2.303 \times I_{corr} \times (\beta_a + \beta_c)} \tag{1}$$

Fig. 4a-b show the polarization curves of TaN coatings. The self-corrosion current density ($I_{corr}$), corrosion potential ($E_{corr}$), cathodic Tafel slope ($\beta_c$), anodic Tafel slope ($\beta_a$), polarization resistance ($R_p$) and corrosion current density at 2 V ($I_{2V}$) are summarized in Table 2. For the TaN coating prepared at $N_2$ flow of 3 sccm, the corrosion resistance of the coating is improved, with the lower $I_{corr}$ of 2.82 $\mu A \cdot cm^{-2}$ and the higher $E_{corr}$ of -0.184 V vs. SCE, because of the lower

roughness (Fig. 2b2) and hydrophobicity (Fig. 2b3). If the $N_2$ flow is further increased to 5 sccm, the corrosion resistance of TaN coatings decreases with the higher $I_{corr}$ of 110.71 $\mu A \cdot cm^{-2}$ and the lower $E_{corr}$ of -0.434 V vs. SCE, as a result of the increased roughness and moresurface defects (Fig. 2a2-d3). Taking into consideration the fact that PEMWE generally works at a higher voltage (> 1.6 V)[14], the corrosion current density at 2 V ($I_{2V}$) is also measured, and the results are displayed in Fig. 4b. The TaN coating prepared at 3sccm $N_2$ flow also exhibits the lowest $I_{2V}$ of 28.5 $\mu A\ cm^{-2}$, but the the corrosion current density at 2 V is 10 times the self-corrosion current density because of the accelerated corrosion at the higher operating voltage of 2 V. Fig. 4c and 4d show the ICR values of TaN coatings. The ICR values decrease with increasing compaction force. The ICR values @ 1.5 MPa

increase with increasing deposition $N_2$ flow, they are 11.48, 21.13, 70.28 and 3227 $m\Omega\cdot cm^2$, respectively , which is significantly lower than that of bare Ti (48.34 $m\Omega\cdot cm^2$). The ICR value @ 1.5 MPa of the TaN coatings prepared at 5 sccm

$N_2$ flow is increased by two orders of magnitude, which might be due to amorphous feature.
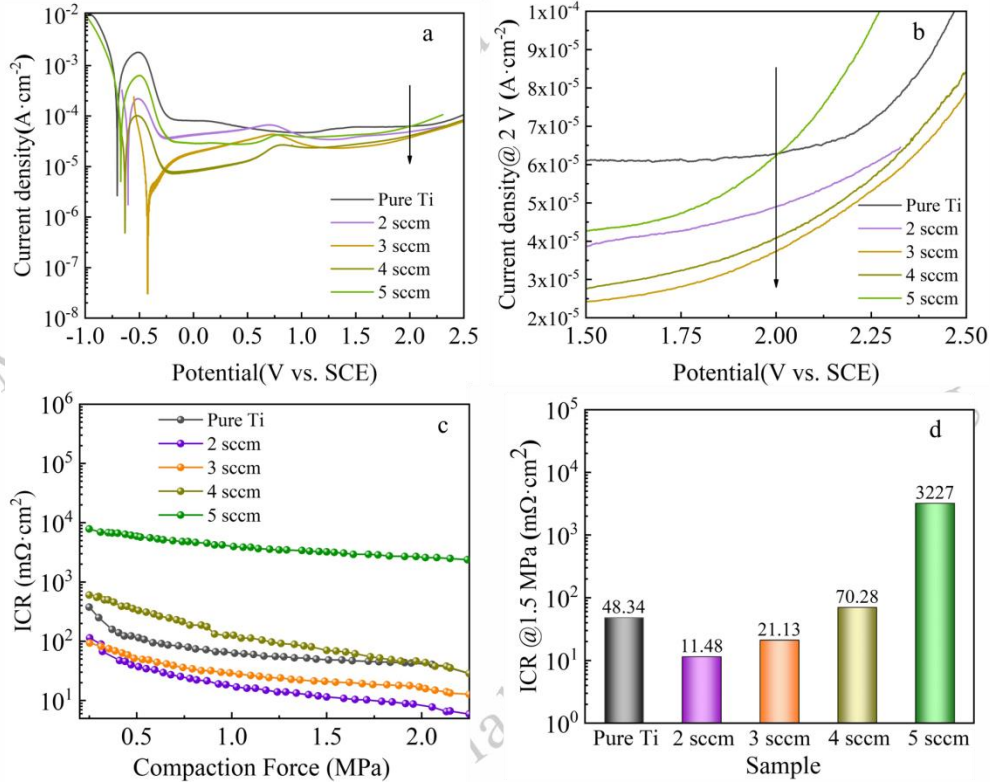


Fig. 4 (a)-(b) Polarization curves of Ti substrate and TaN coatings deposited at different $N_2$ flows, (c) ICR of Ti substrate and the TaN coatings as a function of compaction force, (d) ICR values at the compaction force of 1.5 MPa.

**Table 2 The corrosion data of Ti BPP and TaN coatings at different $N_2$ flows**

| Sample | $E_{corr}$/V vs. SCE | $I_{corr}$/$\mu A\cdot cm^{-2}$ | $I_{2V}$/$\mu A\cdot cm^{-2}$ | $\beta_c$/$mV\cdot dec^{-1}$ | $\beta_a$/$mV\cdot dec^{-1}$ | $R_p$/$\Omega\cdot cm^2$ | $r_{corr}$/$mm\cdot year^{-1}$ |
|---|---|---|---|---|---|---|---|
| Pure Ti | -0.463 | 313.5 | 61.1 | -81.6 | 135.6 | 125 | 3.64 |
| 2 sccm $N_2$ flow | -0.363 | 86.68 | 42.9 | -75.9 | 202.5 | 570 | 1.01 |
| 3 sccm $N_2$ flow | -0.184 | 2.821 | 28.5 | -65.9 | 308.5 | 15758 | 0.033 |
| 4 sccm $N_2$ flow | -0.391 | 23.23 | 32.6 | -51.5 | 136.6 | 1262 | 0.27 |
| 5 sccm $N_2$ flow | -0.434 | 110.7 | 60.04 | -86.3 | 120.7 | 433 | 1.29 |

** $I_{2V}$ is denoted as the corrosion current density at 2 V.

Fig. 5 shows the surface morphology of Ti BPs and TaN coatings after potentiostatic test in the PEMWE simulated acidicaqueous environment (0.5 mol/L $H_2SO_4$ + 2 ppm F⁻) at 2 V and at 80 ℃ for 10 h. As displayed in Fig. 5a, the surface of bare Ti BPs is completely destroyed with obvious titanium grain boundaries after acid corrosion. However, the surface morphology of Ti BPs coated with TaN is well maintained after

potentiostatic polarization at 2 V for 10 h. The corrosion pits increase first and then decrease. Especially, for the TaN coating deposited at 3 sccm $N_2$ flow, fewer corrosion pits are evidenced due to the higher corrosion resistance. For the TaN coatings prepared at 4 and 5 sccm $N_2$ flows, more defects emerge after 10 h potentiostatic polarization test (Fig. 5d and 5e).
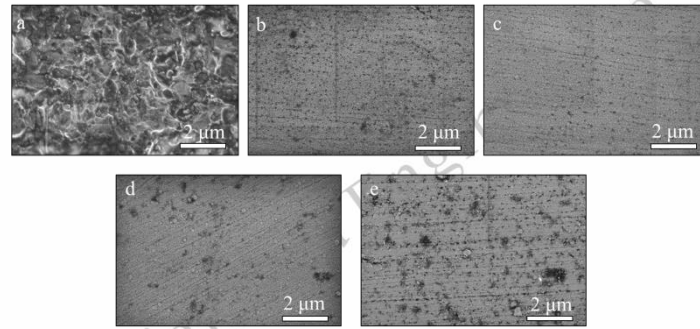
Fig. 5 The surface morphology of Ti and TaN coatings after 10 h potentiostatic polarization test: (a) Ti substrate; TaN coatings prepared at different N₂ flows: (b) 2sccm, (c) 3sccm, (d) 4sccm and (e) 5 sccm.

## 2.5 PEM electrolyser test of TaN coated BPPs

Taking TaN coating deposited at 3 sccm N₂ flow as an example, the coated anode and cathode Ti BPs with an active surface area of 80 cm² are tested in a PEM electrolyser. Fig. 6a shows the polarization curves measured at 80 ℃. The potential of cell assembled with bare Ti BP was 2.472 V at the current density of 2 A·cm⁻². As compared with bare Ti BPs, the electrolytic potential of TaN coated BP is reduced by 323 mV at the current density of 2 A·cm⁻², implying the improved electric conductivity. As a contrast, TiN coatings on Ti sheet[25] and Pt/Ti coatings on stainless steel[26] demonstrates the electrolytic potential of about 2.35 V at 1.5 A·cm⁻² and 2.25 V under 2 A·cm⁻². So the corrosion resistance and electrical conductivity of TaN coatings are higher than those of TiN coatings and Pt/Ti coating. Compared to the thermos-neutral voltage ($V_{tn}$=1.48 V) in the polarization curves, the electrolysis efficiency is determined[27]. At the current density of 1 A·cm⁻², the electrolysis efficiency of the electrolyser increases from 59.87% of Ti BPs to 68.87% of TaN coated Ti BPs, owing to the

reduced ICR between Ti BPs and PTL. Then, the electrolytic cell is tested at a constant current density of 2 A·cm⁻² for 75 h. the electrolytic potential of the bare Ti is rapidly increased above 2.6 V after 35 h, demonstrating the failure of bare Ti bipolar plate. However, the electrolytic voltage of TaN coated Ti BPs is increased slightly from 1.968 V to 2.02 V after 75 h test, as a whole. Comparatively, the electrolytic potential of TiN coatings was increased slight from 2.35 V to 2.37 V under 1.5 A·cm⁻² after 100 h[25], and that of Pt coatings was increased from 1.87 V to 1.875 V under 1.5 A·cm⁻² after 96 h[28]. So the stability of TaN coatings is comparable with those of Pt, but with low cost exhibited a great engineering significance for reducing the cost of bipolar plates. The fluctuations can be ascribed to the temperature fluctuations of circulating water in the electrolytic cell. As displayed in Fig.6b-d, Ti BPs are oxidized and turns yellow after electrolysis test, while TaN coatings on the anode BPs become soft gray as a result of corrosion under saturated O₂ and at higher operating potential.
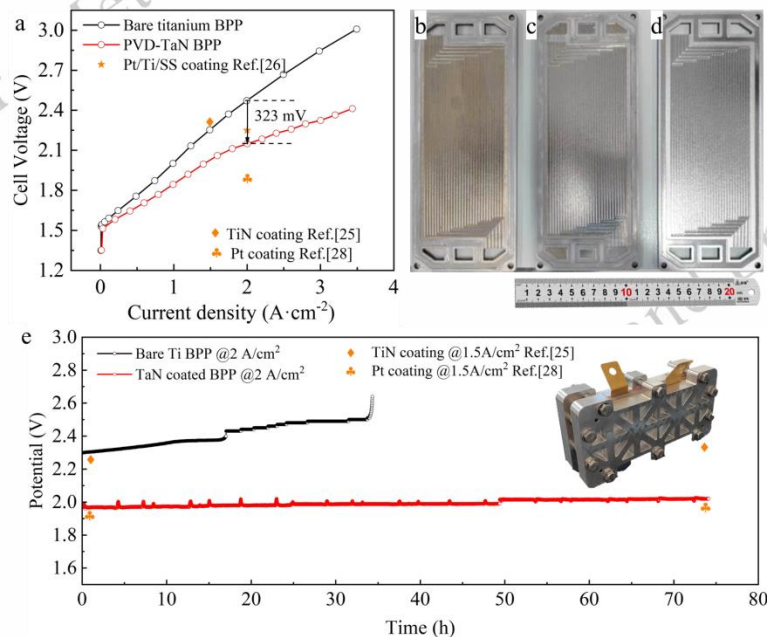


Fig.6(a) The polarization curves of electrolyser assembled with TaN coated and bare Ti BPs; the photographs of Ti BPs after water electrolysis of bare Ti plate (b), anodic TaN coated Ti BPs (c), cathodic TaN coated Ti BPs (d); (e) cell valtages of BPs in single electrolysis cell @2 A·cm⁻² and the test electrolyser in the right inset .

## 3 Conclusion

TaN coatings are prepared on Ti BPs by magnetron sputtering, and the influences of $N_2$ flow on the surface morphology, hydrophobicity, crystallinity, corrosion resistance and interfacial contact resistance of TaN coatings are studied in details. As the $N_2$ flows increases, the surface roughness of TaN coatings decreases first and then increases in accordance with the hydrophobicity of the coatings. The TaN coating prepared at 3 sccm $N_2$ flow presents the lower surface roughness and hydrophobicity. The TaN coating deposited at 5 sccm $N_2$ flow becomes amorphous with many particles on the surface. Consequently, TaN coatings prepared at 3 sccm $N_2$ flow exhibit the best corrosion resistance with the lowest $I_{corr}$ of 2.82 $\mu A \cdot cm^{-2}$ and the highest $E_{corr}$ of -0.184 V vs. SCE. But TaN coatings prepared at 5 sccm $N_2$ flow exhibit the degraded corrosion resistance, and many corrosion pits emerge on the surface after 10 h potentiostatic polarization test. The electrolysis efficiency of the electrolyser is increased from 59.87% of Ti BPs to 68.87% of TaN coated Ti BPs at the current density of 1 $A \cdot cm^{-2}$. Moreover, the TaN coated BPs exhibit the better stability after 75 h water electrolysis at a constant current density of 2 $A \cdot cm^{-2}$ which is comparable with those of Pt, but with low cost exhibited a great engineering significance for reducing the cost of bipolar plates.

## Declaration of Competing Interest

The authors declare that they have no known competing financial interests or personal relationships that could have appeared to influence the work reported in this paper.

## Acknowledgment

## Reference

1 Tao L, You K T, Yan L W *et al. Fuel*[J], 2024, 368:131610.

2 Ibuki S, Koichiro F, Mikito U, Hisayoshi M. *Fusion Engineering and Design*[J], 2024, 202:114420.

3 Yang G, Yu S, Kang Z *et al. Energy Conversion and Management*[J], 2019, 182:108-116.

4 Yuan J L, Jian P G, Qiao M L *et al. The Journal of Physical Chemistry C*[J], 2024, 128:8123-8130.

5 Li W K, Xie Z Y, Zeng H D. *RSC Advances*[J], 2024, 14:7172-7194.

6 Cui Y.F, Cui J.L, Xu X *et al. Fuel Cells*[J], 2017, 17:698-707.

7 Peng F Y, Tao Y, Yao Y *et al. Corrosion Science*[J], 2022, 197:110086.

8 Deng Z, Dai Z, Wu W *et al.Rare Metal Materials and Engineering*[J], 2024, 53(10):2755-2765.

9 Fang Y Y, Bai 1 J, Zi Y W *et al. Materials Chemistry and Physics*[J], 2022, 287:126082.

10 Jun Y C, Sam Z, Jia Z *et al. Journal of Alloys and Compounds*[J], 2024, 976:173033.

11 Mo H C, Ji C D, Se H K *et al. Corrosion Science*[J], 2022, 196:110042.

12 Wen Q S, Yuan J L, Jian P G *et al. Journal of Materials Science & Technology*[J], 2025, 210:86-96.

13 Hai T Z, Dong L G, Hong Z D *et al. Surface and Coatings Technology*[J], 2024, 483: 130769.

14 Fei F B, Pei Y Y, Tao Z *et al. International Journal of Hydrogen Energy*[J], 2015, 40:9790-9802.

15 Gao Y L, Dong F S, Bai Z F *et al. International Journal of Hydrogen Energy*[J], 2023, 48:18996-19007.

16 Haynes W M, David R L, Thomas J B *et al. CRC Hand book of Chemistry and Physics*, 97th ed., CRC Press, 2016.

17 Chang H C, Hyoseok C, Wonhyuk H *et al. International Journal of Hydrogen Energy*[J], 2012, 37:405-411.

18 Lucia M, Anders O, Ole E K *et al. International Journal of Hydrogen Energy*[J], 2017, 42:3259-3270.

19 J.P. Manaud, A. Poulon, S. Gomez, Y.L. Petitcorps. *Surface and Coatings Technology*[J], 2007, 202:222-231.

20 Jian M W, Ji Y Z, *Journal of Alloys and Compounds*[J], 2024,976:173300.

21 Hock C L, Bee H L, Mohd S M *et al. International Journal of Hydrogen Energy*[J], 2024, 57:420-430.

22 Donald H, Hadi A, Andrew R B *et al. Journal of Colloid and Interface Science*[J], 2019, 543:328-334.

[23 Gago A.S, Ansar S.A, Saruhan B *et al. Journal of Power Sources*[J], Mar. 2016,307:815-825.

24 Amin M A, Khaled K F, Fadl-Allah S A. *Corrosion Science*[J], 2010, 52.1: 140-151

25 Toops T J , Brady M P , Zhang F Y *et al. Journal of Power Sources*[J], 2014, 272:954-960

26 Gago A S , Ansar S A , Saruhan B *et al. Journal of Power Sources*[J], 2016,307:815-825

27 Jason K L, Tobias S, Guido B *et al. Applied Energy*[J], 2023, 33:120853.

28 Wang X, Luo H, Cheng H *et al. Applied energy*[J], 2023,357:122517.

# 氮气流量对质子交换膜电解槽双极板上氮化钽涂层微观结构与耐腐蚀性能的影响

高建平 [1,2]，吕源江 [1]，李永婧 [1]，孙雯倩 [1]，任碧莹 [2]，戴正飞 [1]，马飞 [1]

(1. 西安交通大学 金属材料强度国家重点实验室，陕西 西安 710049)

(2. 西部金属材料股份有限公司，陕西 西安 710201)

**摘　要**：腐蚀缩短了双极板（BPs）的使用寿命，并增加了质子交换膜电解槽（PEMWE）的成本。在本研究中，通过磁控溅射在钛基双极板上沉积了 TaN 涂层，以提高其耐腐蚀性和使用寿命，并详细研究了氮气流量对 TaN 涂层的表面形貌、疏水性、结晶度、耐腐蚀性和界面接触电阻的影响。随着氮气流量的增加，TaN 涂层的粗糙度先减小后增大，而疏水性则先增大后减小。在氮气流量为 3 sccm 时，TaN 涂层晶粒较大，呈现出较低的粗糙度和较高的疏水性。在模拟的 PEMWE 环境中，该涂层具有最低的腐蚀电流密度（2.82 μA·cm$^{-2}$）和最高的自腐蚀电位（-0.184 V）。经过 10 h 恒电位极化测试后，在氮气流量为 3 sccm 时沉积的 TaN 涂层上观察到的腐蚀坑较少。经过 75 h 的电解水性能测试，TaN 涂层提高了钛双极板腐蚀电阻进而提高了电解池的电解效率（68.87%），大幅度降低双极板成本。

**关键词**：TaN涂层、耐腐蚀性、钛双极板、水电解

作者简介：高建平，男，1991 年生，博士生，西安交通大学金属材料强度国家重点实验室，陕西西安 710049，电话：15702977035，E-mail: gjp_nwpu@163.com